Journal of Alloys and Compounds 509 (2011) 9363–9371

Contents lists available at ScienceDirect

Journal of Alloys and Compounds

journal homepage: www.elsevier.com/locate/jallcom

Optimization of process parameters for the production of Ni–Mn–Co–Fe based NTC chip thermistors through tape casting route

M.N. Muralidharan, E.K. Sunny, K.R. Dayas, A. Seema*, K.R. Resmi

Centre for Materials for Electronics Technology (C-MET), Athani P.O., Thrissur 680581, Kerala, India

ARTICLE INFO

Article history:
Received 28 February 2011
Received in revised form 11 July 2011
Accepted 13 July 2011
Available online 23 July 2011

Keywords:
Thermistor
Tape casting
Reliability
Sintering

ABSTRACT

Ni–Mn–Co–Fe–O based ceramic compositions were prepared and their NTC thermistor characteristics were evaluated. The tape casting slurry composition was optimized to get defect free ceramic tapes. Chip thermistors were prepared from these NTC tapes by optimizing the process parameters. The prepared chip thermistors were tested for their thermal and electrical reliability and found to have excellent reliability. Tape casting can be employed as an effective and ideal method for the mass production of Ni–Mn–Co–Fe based miniaturized NTC chip thermistors.

© 2011 Elsevier B.V. All rights reserved.

1. Introduction

Temperature monitoring, control and compensation are having great significance in the functioning of majority of domestic and industrial appliances. Thermocouples, resistance temperature detectors (RTDs), integrated circuit (IC) sensors and thermistors are the most widely used temperature sensors in the market [1,2]. Among these, thermistors have found a pervasive role in modern micro electronics due to their unique features like device versatility, stability, good sensitivity, fast response, high productivity, wide range of resistivity, large thermal coefficient and very high degree of accuracy [3]. Applications in advanced areas such as aerospace, cryogenic, medical etc. need thermal sensors with high performance and stability. The long term stability of components is a critical parameter in most temperature sensing and control applications. Moreover, in this era of electronic revolution, sophisticated miniaturized devices with good reliability and capability of withstanding extreme environmental conditions are in great demand. It is an ever demanding criterion of the market to have smaller and smaller devices without a compromise in their performance. Size reduction has many advantages such as fabrication of a large number of devices from a very small quantity of material, lowering the cost of devices, easy handling, small area consumption etc. Chip thermistors are the miniaturized version among the available different shapes of thermistors like discs, rods, washers and beads. In this scenario the development and optimization of process parameters for smaller NTC chip thermistors requires prime importance as their performance, in particular their stability, is strongly dependant on their processing conditions [4].

Ceramic semiconductors exhibiting negative temperature coefficient (NTC) of resistance are the most commonly used materials in the thermistor industry [4–7]. Even though many materials with various crystal structures including spinels, perovskites and pyrochlores exhibit NTC behavior, nickel manganite ($NiMn_2O_4$) with an inverse spinel structure is the most extensively studied NTC thermistor composition. The material constant or *B* value is one of the decisive parameters for selecting an NTC composition for a specific application. Higher commercial demand exists for thermistors having material constant mainly between 3000 K and 5000 K. $NiMn_2O_4$ incorporated with various dopants (e.g. transition metals such as Cu, Co, Fe, Cr etc.) produces NTC materials with various *B*-values which can cater almost all the market requirements.

The ceramic processing technology of tape casting is already in regular use for mass production of miniaturized electronic devices such as multilayer capacitors, actuators etc. [8–11]. This processing method is also adopted for making chip thermistors of smaller sizes [12]. Preparation of a chip thermistor is a multi step process which requires stringent control over process parameters. Although a significant amount of research work has been involved in the area of tape casting, binder removal and sintering of multilayered structures, a systematic study in regard to NTC chip thermistors is important as they are highly sensitive to process conditions.

In tape casting, slurry preparation is a critical step which require precise attention to have defect free, uniform, dense, high quality green ceramic sheets. Tape casting slurry should be a well dispersed homogenous stable system with low viscosity, good shear

* Corresponding author. Tel.: +91 487 2201156; fax: +91 487 2201347.
E-mail addresses: seema@cmet.gov.in, seemaansari@yahoo.com (A. Seema).

0925-8388/$ – see front matter © 2011 Elsevier B.V. All rights reserved.
doi:10.1016/j.jallcom.2011.07.037

Table 1
Molar compositions of samples prepared.

Sample code	Composition (mol)			
	Ni	Mn	Co	Fe
R1	1	1	0.25	0.75
R2	1	1	0.5	0.5
R3	1	1	0.7	0.3
R4	1	1	0.8	0.2
R5	1	1	0.9	0.1

thinning behavior and higher solid loading. The deflocculation of the inorganic ceramic powder is usually achieved by adding suitable type of dispersant in optimum concentration. The mechanism corresponding to dispersion may be electrostatic, steric or a combination of both (electrosteric) [13–15]. Rheological characterization (flow behavior) and sedimentation (settling rate) studies are the well accepted methods for optimizing the amount of dispersant. The system that gives minimum viscosity, a near Newtonian behavior and a lower settling rate implies the best dispersion condition [15–17]. Besides having a well dispersed ceramic powder in the solvent, slurry should contain binder, plasticizers and homogenizer to provide strength and flexibility for tapes after drying [15,18–20].

Thermal compression method is a widely used technique for constructing multilayered ceramic structures from ceramic tapes. Green ceramic tapes are stacked and thermolaminated to get required thickness. Thermolaminating at suitable temperature and pressure results in samples with uniform thickness. The removal of binders from these laminated structures also needs special attention as the final product behavior should not be affected by the tape additives. Binder burn out is a well studied process for the removal of organics in the fabrication of multilayered structures such as capacitors, actuators etc. [21–24].

Negative temperature coefficient behavior of thermistor materials is an effect associated with changes in bulk properties [4,6,7]. Hence sintering process plays a crucial role in molding the behavior of NTC thermistors. The kinetics of sintering process is a well studied phenomenon [25,26]. A lot of research works are there about the influence of sintering process on electrical properties of thermistors [27–31]. Sintering conditions can be adjusted to tailor the electrical properties of the NTC ceramic thermistors.

In the present work, NTC thermistor compositions were prepared from nickel manganite doped with Co_3O_4 and Fe_2O_3. The effect of dopants and the influence of sintering temperature on the electrical properties of this system were already reported on conventional disc type and thick film thermistors [29–32]. Five different compositions of $Ni_1Mn_1Co_xFe_{(1-x)}$ (x = 0.25, 0.5, 0.7, 0.8, 0.9) were synthesized through solid state route. Disc thermistors were made out of these compositions and the NTC thermistor behavior of the system was analysed. The tape casting slurry composition was optimized and chip thermistors were developed through tape casting route. The properties were evaluated and the processing parameters were optimized. The reliability of the chip thermistors was established by thermal and electrical aging studies.

2. Experimental

2.1. Synthesis of NTC compositions

In the present study five different NTC compositions based on $Ni_1Mn_1Co_xFe_{1-x}O_4$ (x = 0.25, 0.5, 0.7, 0.8, 0.9) were prepared by solid state route. The compositions are given in Table 1.

Starting materials such as nickel carbonate basic hydrate, manganese carbonate, Fe_2O_3 and Co_3O_4 (Sigma–Aldrich, USA) were of high purity (>99%) in order to ensure higher quality and reproducibility of the synthesized thermistor compositions. The raw materials were accurately weighed and transferred to polypropylene jars. Using isopropyl alcohol as solvent and yttria stabilized zirconia balls as grinding media the precursors were ball milled for 24 h to get a uniform mix. The powder mix was then calcined at 1173 K for 3 h. The calcined powder was then ground by ball milling for 48 h to achieve a narrow particle size distribution. The slurry after grinding was passed through ASTM 400 mesh size sieve so as to make sure that only particles of uniform size were present in the resulting powder after drying. Crystal structure of the resulting composition was analysed by X-ray diffraction (XRD) (Bruker AXS D5005, Germany). To understand the nature of synthesized NTC powder, scanning electron microscopy (SEM) and particle size analysis (PSA) were also carried out.

2.2. Preparation of disc thermistors

The NTC powder after grinding was granulated using 5% PVA solution and green discs of 10 mm diameter and 1.7 mm thickness were prepared by uniaxial compaction. The green body was then sintered at 1473 K or 1523 K for 3 h and slowly cooled. Sintered discs were electroded using silver paste (Shoei – H-5698, Japan) and fired by passing it through a conveyor belt furnace with a peak temperature of 1023 K. The speed of the conveyor was adjusted so as to keep the sample at the peak temperature for 10 min. After curing, the discs were kept at a temperature of 393 K for two days, to ensure thermal stability.

2.3. Tape casting studies for thermistor compositions

The slurry of the tape casting process was prepared in xylene–ethanol (50:50 ratio) solvent system with different dispersants viz. KD1 (a copolymer of poly ester and poly amide, Tape Casting Warehouse, USA), PE (phosphate ester, Tape Casting Warehouse, USA) and MFO (menhaden fish oil, Tape Casting Warehouse, USA). For optimizing the dispersant and its concentration, dispersion studies (sedimentation and rheological characterization) were conducted using systems with 33 wt% solid content. The slurry containing dispersant, powder, solvent and grinding media was ball milled for 4 h before conducting dispersion studies. For sedimentation study, 10 ml of the slurry was transferred to a graduated measuring cylinder and allowed to settle. The settling rate against time was noted. In rheological characterization rheometer (Brookfield Programmable DVIII + Rheometer) with UL adaptor was used. The general behavior of the slurry was studied by plotting the variation of viscosity with shear rate.

With optimum amount of dispersant, tape casting slurry was prepared in double step process. In the first step dispersant was added along with powder and balls in the solvent system and ball milled for 6 h. In the second stage, plasticizers, binder and homogenizer were added and ball milled for 17 h followed by 1h slow ball milling. Polyethylene glycol 400 (PEG, Merck, India) and benzyl butyl phthalate (BBP, Sigma–Aldrich, India) were used as the plasticizers. A 22 wt% solution of poly vinyl butyral-co-vinyl alcohol-co-vinyl acetate (PVB, MW 70,000–100,000, Sigma–Aldrich, India) in ethanol was used as binder and cyclohexanone (Merck, India) as the homogenizer. Using double doctor blade technique in a laboratory batch type caster (E.P.H. Engineering, USA) the slurry was casted on a clean glass plate at 293 K and allowed to dry. The blade gap was adjusted to 400 μm to have a tape of 120 ± 5 μm thickness.

2.4. Preparation of NTC chip thermistors

1 inch × 1 inch square pieces were punched out from the green tape and were stacked one over the other to get desired thickness. They were thermolaminated at a temperature of 363 K and a pressure of 120 kg/cm^2 for 2 h.

The green thermolaminated sample contains a lot of organic additives which have temporary function in this process. These must be eliminated before densification starts. As the green tape have a relatively high packing density of particles, a controlled burning of binders from the tape is required to avoid damages like delamination, cracks etc. This is because the loss of binders is not at a constant rate. Different additives have different volatile rates. To optimize the binder burn out condition thermal analysis of the green tape was done by differential scanning calorimetry and thermo gravimetric analysis (DSC/TGA) (Perkin Elmer, Diamond DSC/TGA, USA) at a heating rate of 10 °C per min in air atmosphere. From the thermal analysis data the rate of removal of volatiles was understood. Through precisely controlled heating cycle almost complete thermal degradation of binders (~97%) was achieved. Intermittent air flow was given to facilitate easy removal of the volatile materials.

The sample after binder bun out was sintered at different sintering conditions in air and cooled very slowly. Setter plates (which were made by mixing 20 wt% of NTC powder with Calcia stabilized Zirconia powder) were placed above the sample before sintering so as to avoid warpage. The sintered samples were polished and electroded by screen printing in a screen printing machine (Keko P-200SL, Haikutech, Netherlands) using the same silver paste as used in the case of disc thermistors. Further process of curing and aging was done as same as that of disc thermistors. After aging, samples were diced into 1 mm × 1 mm size chip thermistors using dicing machine (ADT 7100 Vectus+, Israel).

2.5. Electrical characterization and reliability studies

Electrical resistance of the disc and chip samples were measured at 298 K and 358 K in a constant temperature silicon oil bath (Model 7340, Hart Scientific, USA) with a temperature uniformity of ±0.005 °C, using a precise digital multimeter (Fluke 8808A, USA) with 0.03% dc current accuracy. The characteristic parameters

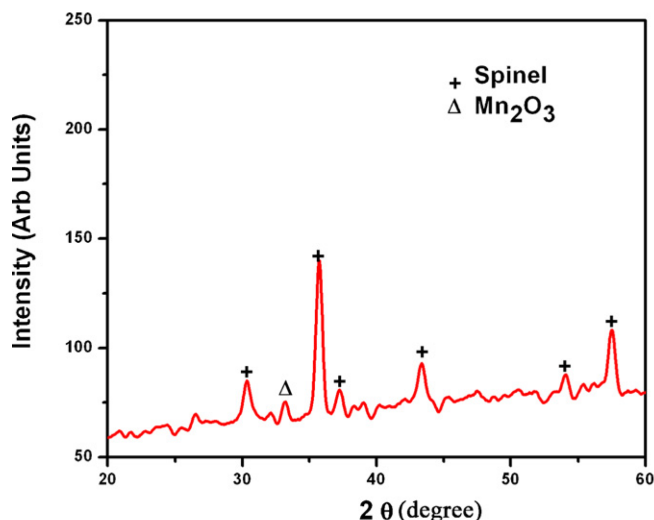

Fig. 1. XRD pattern of the composition $Ni_1Mn_1Co_{0.7}Fe_{0.3}O_4$ calcined at 1173 K.

of a thermistor such as material constant, temperature coefficient of resistance and activation energy were calculated from these values.

The chip thermistors were subjected to thermal as well as electrical reliability studies. The resistance values (at 298 K) of chips before and after the test were measured. The percentage drift in resistance values after the tests is taken as the measure of its reliability. The thermal aging studies were carried out in thermal cycling equipment (Vijayalakshmi Industries, India). The chips were subjected to thermal shock by rapidly moving between a cold and a hot chamber kept at 218 K and 423 K respectively, for 100 cycles. The retention time at each chamber was 30 min. In the electrical aging studies, chip samples were given a power of 60 mW for 100 h using a source meter (Keithley 2400, USA). The resistance measurements of NTC chips at 298 K were again carried out and drift in resistance was calculated.

3. Results and discussions

3.1. Analysis of NTC behavior of compositions $Ni_1Mn_1Co_xFe_{(1-x)}O_4$

The X-ray diffraction pattern of the composition $Ni_1Mn_1Co_{0.7}Fe_{0.3}O_4$ calcined at 1173 K is shown in Fig. 1. From the XRD pattern, when compared with standard (ICDD file No. 01-1110), it was found that, besides the spinel phase there is also a Brag reflection corresponding to Mn_2O_3. It is well known from the phase diagram of Ni–Mn–O system [33] that only the compositions with Ni/(Ni + Mn) ratio less than 0.35 can form phase pure spinel structure at a calcination temperature of 1173 K. But in the present system, the Ni/(Ni + Mn) ratio is more than 0.4 and it is well expected to find an additional phase of Mn_2O_3.

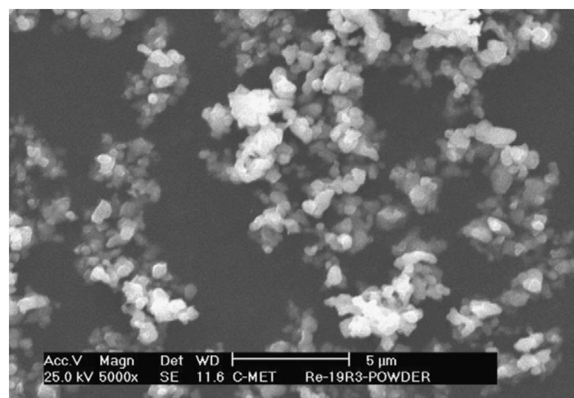

Fig. 3. SEM image of $Ni_1Mn_1Co_{0.7}Fe_{0.3}O_4$ NTC powder.

Particle size and their distribution affect the physical properties of powders, such as packing density, porosity, fired shrinkage and firing range [2]. PSA analysis report of composition R3 is given in Fig. 2. This analysis shows that the ground calcined powder of the composition show an average particle size of around 1.75 μm and a narrow particle-size distribution. The SEM image (Fig. 3) of the ground-calcined powder shows agglomerated particles with a uniform particle-size distribution, which supports the PSA analysis. The narrow particle-size distribution of the NTC powder resulted in the higher sintered density (96–98% theoretical) of the final product.

As the NTC behavior of ceramic semiconductors is a grain phenomenon, densification plays a key role in the properties of NTC thermistors. Among the sintering conditions, sintering temperature, rate of heating, rate of cooling and dwell time are important factors to be controlled [8,28,29,34,35]. In this study a cooling rate of 2 °C per min was applied after sintering, to minimize thermal shock stresses. All the sintered discs showed a linear shrinkage of 15–19% and volume shrinkage of 35–40%.

Fig. 4 shows the SEM images of disc thermistors sintered at 1523 K. It was found that, in all the compositions proper densifications has taken place (96–98% of the theoretical density was achieved for all the compositions) and have similar type of grains. However, as the Co content increases, precipitation of secondary phase on the grains is observed.

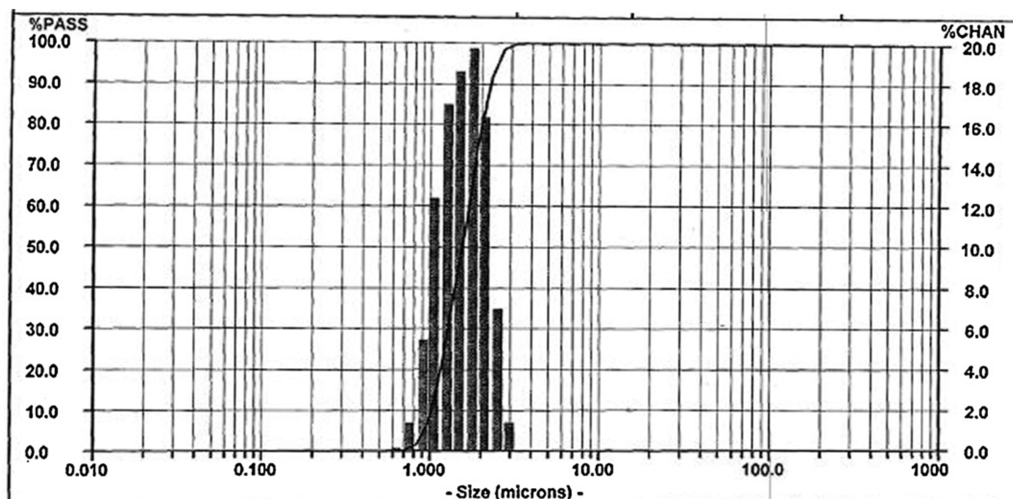

Fig. 2. Particle size distribution of the $Ni_1Mn_1Co_{0.7}Fe_{0.3}O_4$ NTC powder.

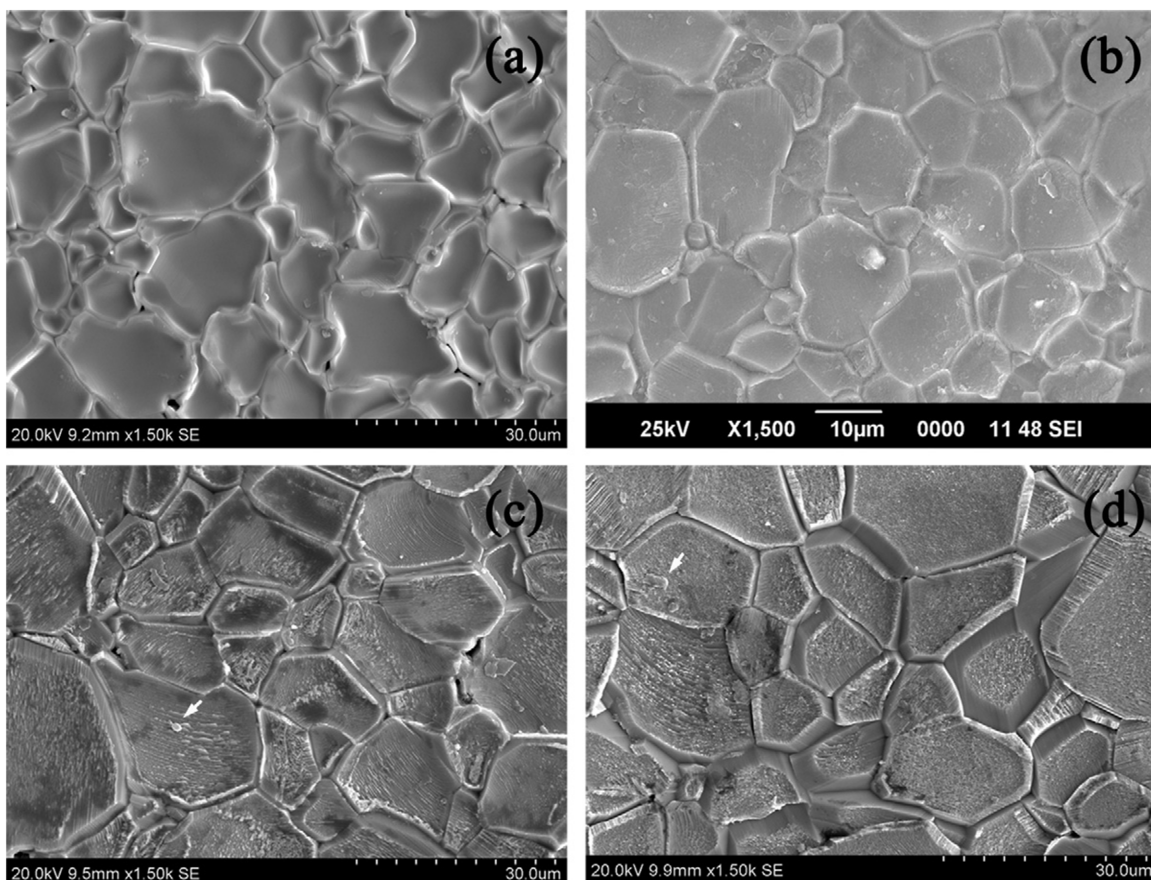

Fig. 4. SEM image of NTC Discs sintered at 1523 K (a) $Ni_1Mn_1Co_{0.5}Fe_{0.5}O_4$, (b) $Ni_1Mn_1Co_{0.7}Fe_{0.3}O_4$, (c) $Ni_1Mn_1Co_{0.8}Fe_{0.2}O_4$ and (d) $Ni_1Mn_1Co_{0.9}Fe_{0.1}O_4$.

The main electrical characteristics of NTC thermistors are, room temperature resistivity (ρ_{298}), material constant (*B*-value) and temperature coefficient of resistance (α). The electrical parameters, *B*-value and 'α' can be derived from the resistance temperature characteristics. These parameters determine the condition under which a given thermistor material may be utilized [4,7]. The resistance (*R*) and temperature (*T*) relationship of an NTC thermistor can be represented as Eq. (1):

$$R = A\ \exp\left(\frac{q}{kT}\right) \tag{1}$$

where *A* is a constant related to the device dimensions and resistivity (ρ). '*q*' is the activation energy for the hopping process and '*k*' is Boltzmann's constant. *B*-Value is simply 'q/k' and is usually calculated using the following Eq. (2):

$$B_{298/358} = \left(\frac{T_{298}T_{358}\ \ln(R_{298}/R_{358})}{T_{298} - T_{358}}\right) \tag{2}$$

where R_{298} and R_{358} are the resistance values at 298 K (T_{298}) and 358 (T_{358}) respectively. The temperature coefficient of resistance (α) is defined as the rate of change of resistance (*R*) with temperature (*T*) to the resistance at a specified temperature and is given by Eq. (3):

$$\alpha_{298} = \left(\frac{(1/R)\,dR}{dT}\right) = -\frac{B}{T^2} \tag{3}$$

Fig. 5 shows a linear dependence of log ρ versus $1/T$ over a wide temperature range for the aged disc thermistors, which is an indication of good NTC thermistor characteristic. The main electrical characteristics of the developed compositions sintered at 1523 K are listed in Table 2

The table shows the values of material constant obtained for samples sintered at 1523 K. The *B*-value varies from 3253 K to 3563 K. These values are with in the requirements of the industry (3000 K and 5000 K) for NTC thermistors. Analyzing the results, the resistivities of compositions were found to be increasing with increase in Fe_2O_3 content. This indicates that added Fe_2O_3 content causes an increase in resistivity. At a given Ni–Mn content, the

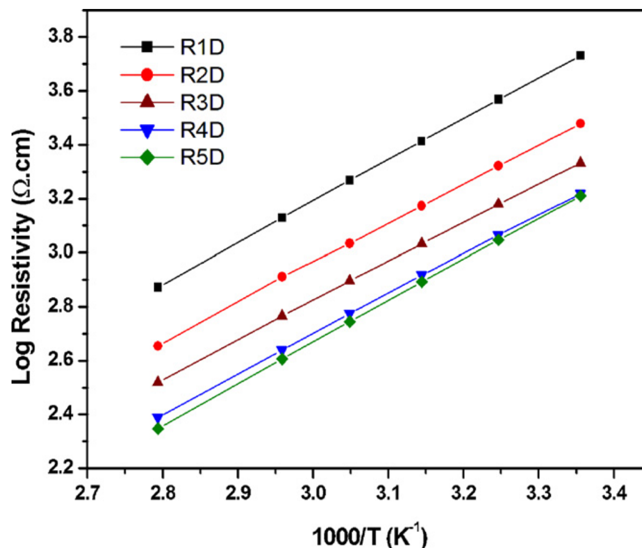

Fig. 5. Relationship between log ρ and reciprocal of absolute temperature ($1/T$) for disc thermistors, (R1D) $Ni_1Mn_1Co_{0.25}Fe_{0.75}O_4$; (R2D) $Ni_1Mn_1Co_{0.5}Fe_{0.5}O_4$; (R3D) $Ni_1Mn_1Co_{0.7}Fe_{0.3}O_4$; (R4D) $Ni_1Mn_1Co_{0.8}Fe_{0.2}O_4$; (R5C) $Ni_1Mn_1Co_{0.9}Fe_{0.1}O_4$.

Table 2
Electrical characteristics of $Ni_1Mn_1Co_xFe_{(1-x)}O_4$ disc thermistors sintered at 1523 K with a heating rate of 2 °C/min and 180 min dwell time.

Sample code	$B_{298/358}$ (K)	Resistivity at 298 K (Ω cm)	Activation energy, q (eV)	Temperature coefficient of resistance (α_{298}), (%/K)
R1	3563	7245	0.3073	-4.01
R2	3463	3906	0.2987	-3.89
R3	3253	2277	0.2806	-3.66
R4	3377	1711	0.2913	-3.80
R5	3424	1396	0.2953	-3.86

activation energy and temperature coefficient of resistance of thermistors is higher for the composition having high Fe_2O_3 content. In the case of nickel manganite spinels conductivity depends on the change in concentration and ordering of the hopping charge carriers namely Mn^{3+} and Mn^{4+} at octahedral sites. Using Mossbauer technique several authors investigated the distribution of 'Fe' ions in the thermistors [36,37]. Studies shows that iron exist as Fe^{2+} and Fe^{3+} in the tetrahedral and octahedral sites of the nickel manganite spinel [30]. According to dilution principle, Fe^{3+} substitution does not change the valence of Mn^{3+}, it changes only the hopping distance between the charge carriers Mn^{3+}/Mn^{4+} [38]. Therefore the presence of foreign ion on the octahedral sites may distract the conduction process. Moreover, with an increase in Fe_2O_3 content, cobalt content in the octahedral site decreases. This decrease leads to a reduction in ions capable of either donating or accepting of electrons in the electron transfer and thus an increase in the resistivity [29]. These changes effectively reduce hopping probability, leading to an increase in activation energy of hopping and thereby an increase in resistivity.

3.2. Effect of dispersants and optimization of tape casting slurry

Initially in the tape casting process, slurry of the composition was prepared in a binary solvent system (xylene–ethanol, 50:50). Multiple solvent system has many advantages such as increased ability to dissolve other organic additives (such as binders, plasticizers) greater control over drying speed, rheological control, cost and safety [13].

The degree of dispersion of the ceramic slurry is usually determined by rheological characterization and sedimentation studies. Rheological characterization involves the study of viscosity of slips under different shearing conditions. These viscosity data were analysed using Casson's mathematical model with Rheocalc software. Casson's equation is:

$$\tau = (\tau_0)^{1/2} + (\eta D)^{1/2} \quad (4)$$

where τ: shear stress, τ_0: yield stress, η: viscosity, D: shear rate.

The yield stress "τ_0" is an important parameter which defines whether a system is well dispersed or not. This parameter gives the minimum tension necessary to cause flow and helps to compare quantitatively the flow behavior of different slurries. Generally lower viscosities and lower yield stress indicate stable system. Table 3 shows the yield stress for NTC slurry with various dispersants. The system with KD1 as the dispersant gives minimum yield stress compared to other dispersants.

Table 3
Yield stress for systems having different dispersant.

Dispersant	Yield stress (dynes/cm^2)
Powder slurry (with out dispersant)	2.14
KD1	0.03
Phosphate ester	0.05
Menhaden fish oil	0.65

The rheological behavior of the slurry with various dispersants is shown in Fig. 6. From the figure it is clear that slurry with KD1 as dispersant has lower viscosity. This is supported by the data given in Table 3 which shows slurry with KD1 as dispersant has lower yield stress. The lower viscosity and lower yield stress are the indications of a well dispersed slurry. Of the added dispersants, PE (phosphate ester) is an electrostatic dispersant and MFO (menhaden fish oil) is a steric dispersant while KD1 is an electrosteric dispersant which combines the action of both electrostatic and steric dispersants. In the slurry KD1 dissociates to positively charge long chains, which adsorb on the surface of the particle and forms the electrostatic and steric hindrance [39]. These two mechanisms together provide better stability to the system. Thus KD1 is an effective dispersant for this kind of NTC ceramic slurry.

For determining the amount of KD1 in the slurry, rheological and sedimentation studies were carried out with different weight percentage of the dispersant. In the sedimentation technique the rate at which the dispersed powder settles under gravity, gives a visual indication of the state of dispersion and stability. Lower settling rate gives better stability. The settling rate in the first 1 h of the NTC slurry with various amounts of KD1 is shown in Fig. 7. From the figure it is clear that slurry containing 1% KD1 as dispersant has lower rate of settling.

In the rheological characterization, viscosity against shear rate for different amount of dispersants is plotted and it is given in Fig. 8. Yield stress for these systems is given in Table 4

From Fig. 8 and Table 4 it is clear that slurry having 1% dispersant have lower viscosity and yield stress, which is essential for a good tape casting slurry. This result supports the sedimenta-

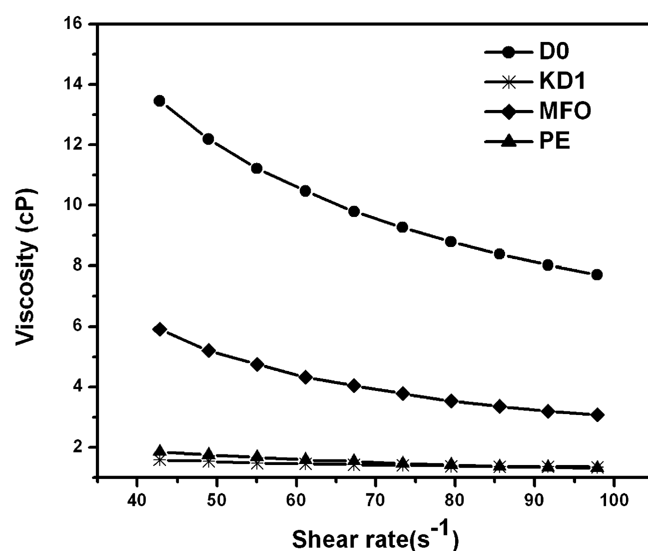

Fig. 6. Graph showing variation of viscosity with shear rate for various dispersants.

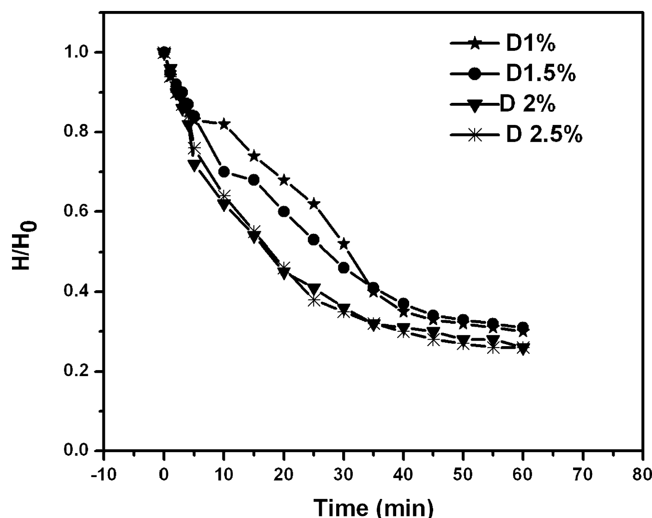

Fig. 7. Relative sedimentation height with time for various amounts of KD1 as dispersant.

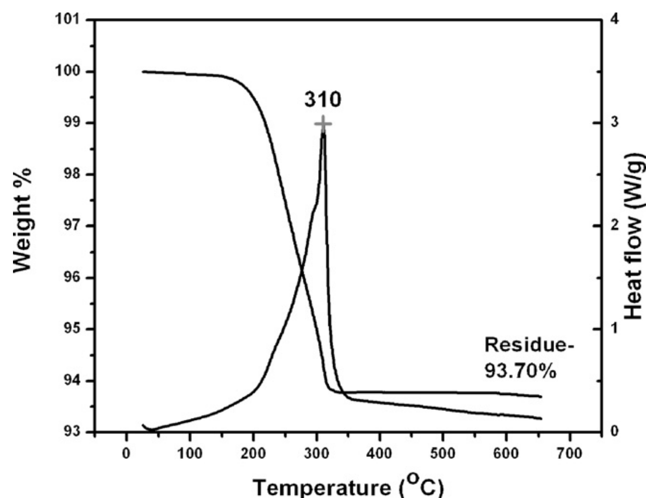

Fig. 9. DSC–TGA curve of the green tape.

Table 4
Yield stress for systems having different amount of KD1 as dispersant.

KD1 (wt%)	Yield stress (dynes/cm^2)
0	2.14
0.5	0.07
1	0.03
1.5	0.04
2	0.04
2.5	0.03

tion results for 1% dispersant. Hence 1% dispersant is found to be the optimum amount for the present NTC system. The slurry also shows a decrease in viscosity with increasing shear rate. This indicates shear thinning behavior which is essential for thick slurry to spread during casting [12].

With optimum amount of dispersant, the final tape casting slurry was prepared by adding binder, homogenizer and plasticizers. Solid loading increased to a level of 66% for these systems. For providing flexibility to the tape, a combination of two plasticizers (PEG and BBP) was used in this study [11]. Cyclohexanone was

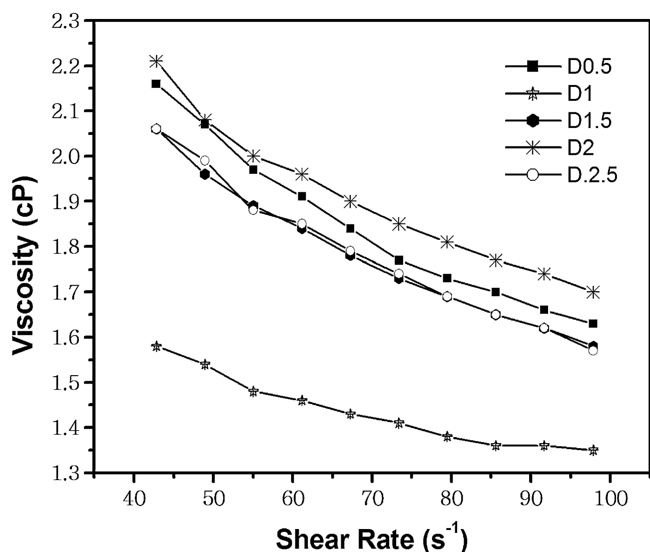

Fig. 8. Graph showing variation of viscosity with shear rate for various amounts of KD1 as dispersant.

used as homogenizer (which retards the skin formation) and PVB as binder. Binders usually form a net work that holds the entire system together for further processing. To get tapes free from visible defects, by keeping the amount of homogenizer and solid loading constant, the binder to plasticizer ratio was varied. The results are given in Table 5

The optimized tape slurry composition for getting a defect free tape is shown the Table 6. Analyzing the quality of tapes it was found that binder to plasticizer ratio is critical in obtaining good quality tapes [12]. Results also indicate that higher amount of powder loading with optimum amount of binder and plasticizer made the slurry too thick to spread. With optimized tape casting slurry, a green body having higher green bulk density and uniformly distributed particles was obtained after casting and drying.

3.3. Thermolamination and binder burn out

In order obtain desired thickness, 1 in. × 1 in. square pieces of green tapes were stacked one over the other and thermolaminated to get a multilayered structure of uniform thickness. The temperature and pressure applied to get maximum compaction and green density was 363 K and 120 kg/cm^2 pressure respectively. Pressure applied during thermolamination ensures a thorough interpenetration of powder particles in the constituent tape and the temperature softens the binder, causing the adhesion and interpenetration of the tapes easier.

Among the organic additives present in the sample, solvents and homogenizer evaporates at the time of drying itself. The remaining dispersant, binder and plasticizers were eliminated by a binder burn out process. DSC–TG analysis was used to find out the thermal properties of the green tape. The DSC–TGA curve for the green tape is given in Fig. 9. Approximately 6.3% weight loss was observed on heating which closely matches with the calculated weight loss for the removal of additives. The decomposition temperature range of volatiles was shown in the exothermic curve of DSC analysis. Most of the volatiles decompose in the temperature range of 423 and 633 K. The binder burn out heating cycle was determined according to this thermal analysis. A very slow rate of heating (6 °/h) was given at the decomposition temperature range. Intermittent air flow was given at different stages, to aid the removal of organics from the tape [25]. The experimental weight loss on binder burn out process was approximately 97% of the theoretically calculated weight loss for the removal of additives. This indicates that, by a controlled binder burn out cycle, complete thermal degradation of

Table 5
Effect of the slip additives in tape characteristics.

Sl. no.	Homogenizer (%)	Binder/plasticizer ratio	Solid loading (%)	Tape characteristics
1	0.94	2.84	66	Rain drop
2	0.94	3.09	66	Rain drop
3	0.94	3.33	66	Rain drop
4	0.94	3.63	66	Good
5	0.94	3.63	68	Too thick slurry

Table 6
Optimized wt% of various additives of tape casting slurry.

Constituents	Role of constituent	wt%
KD1	Dispersant	0.63
Xylene	Solvent	16.16
Ethanol	Solvent	16.16
NTC composition	Ceramic powder	62.76
Cyclohexanone	Homogenizer	0.94
Poly ethylene glycol	Plasticizer	0.31
BBP	Plasticizer	0.41
PVB	Binder	2.6

the tape additives with out remaining any carbon residue in the NTC specimen is possible.

3.4. Effect of sintering conditions on electrical properties

The NTC thermistor slabs, after binder burn out, were sintered at high temperatures. This densification process plays an important role as it determines the final characteristics of NTC chip thermistors. A cooling rate of 2 °C/min was given after sintering as in the case of disc thermistors. All the sintered chips showed a linear shrinkage of 15–20% and a volume shrinkage of 35–40%. About 96–98% of theoretical density was achieved experimentally. The electroded chip samples were diced into 1 mm × 1 mm × 0.5 mm size and electrical measurements were carried out.

In order to understand the effect of sintering temperature on the electrical properties of the chip thermistors, the thermistor samples were sintered at different temperatures by keeping the heating rate, cooling rate and the dwell time constant. The electrical properties at different sintering temperatures are given in Table 7.

It was observed that, there is an increase in activation energy, resistivity and hence *B*-value with increase in the sintering temperature up to 1523 K and there after it becomes almost constant. As the sintering temperature increases, oxygen loss from the sample can also take place, which changes the cation distribution in the spinel and the loss of one molecule of divalent oxygen will reduce two molecules of Mn^{4+} to Mn^{3+}, hence decreases the hopping probability [40]. These spatial changes decrease the probability of hopping mechanism. The segregation or precipitation of impurities and additives at grain boundaries may form potential barriers, which also induce an increase in resistivity [6,41] and in the activation energy. But, as the sintering temperature increases, the effect of larger grain size also comes in to play. The effect of grain boundary scattering on electrical conduction process can be neglected for large grain sized ceramics [42] and hence there is a decrease in activation energy which nullifies the oxygen loss effect and thus gets leveled off. Hence on increasing sintering temperature, the activation energy increase up to a maximum and the electrical properties reach a saturation level. Further increase in temperature may cause melting of the specimen.

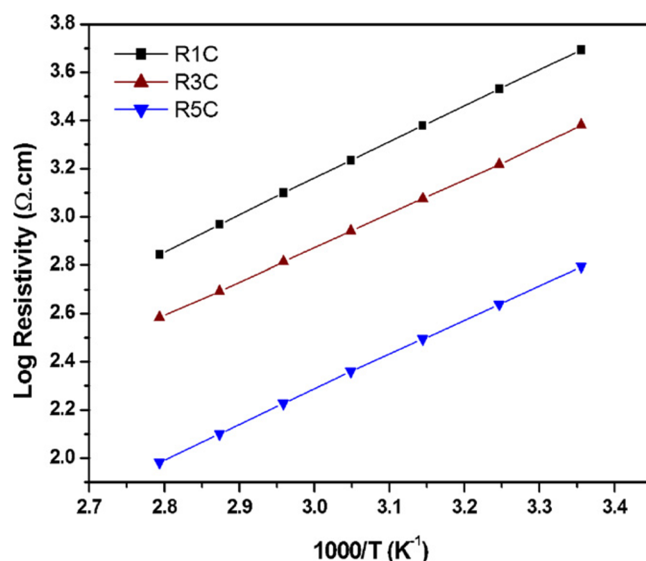

Fig. 10. Relationship between log ρ and reciprocal of absolute temperature ($1/T$) for. chip thermistors, (R1C) $Ni_1Mn_1Co_{0.25}Fe_{0.75}O_4$; (R3C) $Ni_1Mn_1Co_{0.7}Fe_{0.3}O_4$; (R5C) $Ni_1Mn_1Co_{0.9}Fe_{0.1}O_4$.

Fig. 10 shows the linear dependence of log resistivity versus $1/T$ for the aged chip thermistors, which is an indication of good NTC thermistor characteristic [2–4,6,7]. Table 8 shows a comparison of electrical properties and sintering conditions of disc and chip thermistors of the composition $Ni_1Mn_1Co_{0.7}Fe_{0.3}O_4$. Similar electrical properties were achieved in both chip and disc thermistors for different sintering conditions.

NTC chips (400 mm^2 area and 0.5 mm thickness) require shorter dwell time than disc thermistors (200 mm^2 area and 1.5 mm thickness). Also the rate of heating is higher for chip thermistors to get similar electrical properties of NTC discs. This is mainly because of the higher surface area and smaller thickness of the chip thermistors, which makes the thermal conduction easier. The mechanism of grain formation and grain growth requires less time in the isothermal condition than in the case of disc thermistors. The NTC chip thermistors were cracked when they were sintered at the

Table 7
Electrical characteristics of $Ni_1Mn_1Co_{0.7}Fe_{0.3}O_4$ NTC chips sintered at different temperatures with a heating rate of 2.5 °C/min and 30 min dwell time.

Sintering temperature (K)	Sample code	$B_{298/358}$ (K)	Resistivity at 298 K (Ω cm)	Activation energy, q (eV)	Temperature coefficient of resistance (α_{298}) (%/K)
1403	RK1	2920	619	0.2519	−3.29
1473	RK2	3037	847	0.2619	−3.42
1523	RK3	3097	1016	0.2671	−3.49
1573	RK4	3085	1051	0.2661	−3.47
1623	RK5	3110	1246	0.2682	−3.50

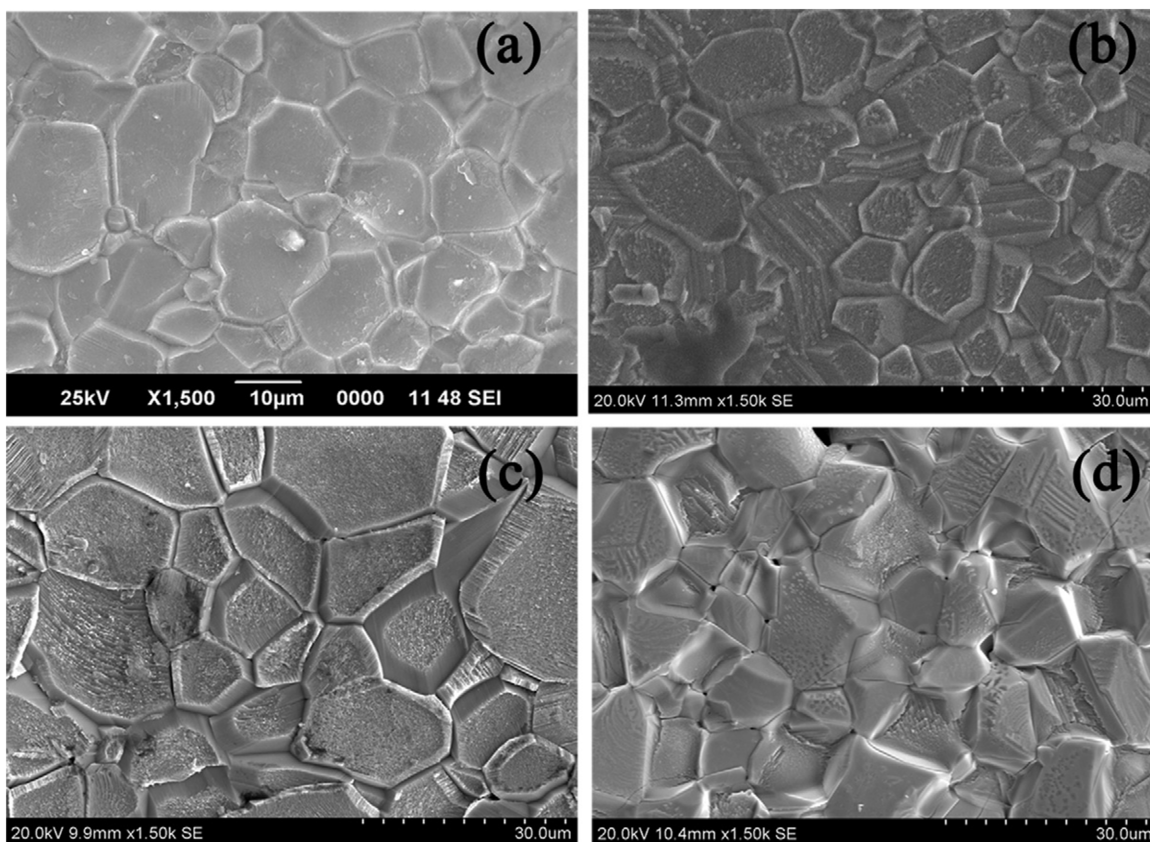

Fig. 11. SEM image of NTC Disc and Chip thermistors. (a) $Ni_1Mn_1Co_{0.7}Fe_{0.3}O_4$ disc, (b) $Ni_1Mn_1Co_{0.7}Fe_{0.3}O_4$ chip, (c) $Ni_1Mn_1Co_{0.9}Fe_{0.1}O_4$ disc, (d) $Ni_1Mn_1Co_{0.9}Fe_{0.1}O_4$ chip.

Table 8
Electrical characteristics of disc and chip thermistors of the composition $Ni_1Mn_1Co_{0.7}Fe_{0.3}O_4$.

Thermistor type	Sintering temperature (K)	Dwell time (min)	Rate of heating (°C/min)	$B_{298/358}$ (K)	Resistivity at 298 K (Ω·cm)	Temperature coefficient of resistance, α_{298} (%/K)	Activation energy, q (eV)
Disc	1523	180	2	3253	2277	– 3.66	0.2806
Chip	1533	60	3.5	3248	1909	– 3.65	0.2801

same dwell time (180 min) as in the case of disc thermistors. This is because, at longer isothermal conditions the grain growth becomes higher and they may begin to fuse.

The SEM images of disc and chip thermistors are compared in Fig. 11. The disc thermistors were sintered for 3 h. whereas the chip thermistors were sintered for 30 min only at the same temperature. It can be clearly observed that microstructures similar to that of disc thermistors can be achieved for chip thermistors by sintering for a shorter duration than that of disc thermistors.

3.5. Reliability of chip thermistors

The NTC chip thermistors were tested for their reliability by thermal and electrical aging. In thermal aging studies thermal

Table 9
Thermal and electrical aging results of chip thermistors.

Reliability test	Sl No.	Initial reading R_{298} (kΩ)	Final reading R_{298} (kΩ)	Drift in resistance (ΔR) (%)
Thermal aging	A1	9.987	10.0376	0.51
	A2	10.589	10.5957	0.06
	A3	9.999	10.0061	0.07
	A4	10.180	10.1835	0.03
	A5	10.591	10.5981	0.07
	A6	10.352	10.3858	0.33
	A7	9.950	9.9536	0.04
	A8	9.963	9.9652	0.02
Electrical aging	A9	10.387	10.268	1.16
	A10	10.684	10.481	1.9
	A11	10.963	10.842	0.86

cycling experiment over 100 cycles was carried out. Percentage drift in resistance was calculated. The results are summarized in Table 9. The result shows a resistance drift less than +0.55% for all the chip thermistors. This indicates an excellent reliability of $Ni_1Mn_1Co_{0.7}Fe_{0.3}O_4$ NTC chip thermistors compared to the low reliability of Ni–Mn–Fe–O system (ΔR of greater than +1%) [43].

To check the capability of withstanding extreme electrical conditions, electrical aging study was also carried out. Chip samples were given a power of 60 mW for 100 h. Again the electrical resistance (R_{298}) measurements were repeated and drift in resistance (ΔR) was calculated. In this case the resistance change was less than −2% for all chip thermistors. This also indicates that the developed chip thermistors can overcome electrical stresses.

4. Conclusion

The synthesized ceramic composition Ni–Mn–Co_x–$Fe_{(1-x)}O_4$ (x = 0.25–0.9) exhibited an excellent NTC thermistor behavior. Through tape casting route NTC chip thermistors were fabricated. The dispersion nature of the thermistor slurry was studied systematically. The type and amount of dispersant was optimized through rheological characterization and sedimentation studies. 1% KD1 was found to be optimum for this thermistor composition. With optimum amount of dispersant and other organic additives defect free NTC tapes were obtained.

By uniaxial thermo compression method, a uniformly laminated specimen for fabrication of NTC chips was obtained. With controlled binder burn out cycle almost complete removal of organics from laminated sample was achieved. Densification provided flexibility in tailoring the electrical properties of chip thermistors. With appropriate sintering conditions the properties of disc thermistors was also obtained on smaller size chip thermistors. Furthermore chip thermistors shows a resistance drift of less than +0.55% after thermal aging and less than 2% after electrical aging, an indication of excellent stability of the fabricated device.

In general, this work could establish that the ceramic processing route of tape casting is an ideal method for the mass production of Ni–Mn–Co–Fe based miniaturized NTC chip thermistors with excellent reliability.

Acknowledgement

The authors gratefully acknowledge Department of Information Technology, Government of India for financial support.

References

[1] A. Feteira, J. Am. Ceram. Soc. 92 (2009) 967–983.
[2] J.M. Varghese, A. Seema, K.R. Dayas, Mater. Sci. Eng. B 149 (2008) 47–52.
[3] E.S. Na, U.G. Paik, S.C. Choi, J. Ceram. Process. Res. 2 (2001) 31–34.
[4] E.D. Macklen, Thermistors, Electrochemical Publications Ltd., Scotland, 1979.
[5] E.J.W. Verwey, P.W. Haayman, F.C. Romeijn, G.W. Vanoosterhout, Philips Res. Rep. 5 (1950) 173–187.
[6] J.G. Fagan, V.R.W. Amarakoon, Am. Ceram. Soc. Bull. 72 (1993) 70–79.
[7] D.C. Hill, H.L. Tuller, in: R.C. Buchanan (Ed.), Ceramic Materials for Electronics, Marcel Dekker, New York, 1986, pp. 249–302.
[8] E.P. Hayatt, Am. Ceram. Soc. Bull. 65 (1986) 637–638.
[9] R.E. Mistler, Am. Ceram. Soc. Bull. 77 (1998) 82–86.
[10] R.E. Mistler, Ceram. Trans. 97 (1999) 87.
[11] R.E. Mistler, E.R. Twiname, Tape Casting Theory and Practice, American Ceramic Society, Westerville, 2000.
[12] N.P. Prasanth, J.M. Varghese, K. Prasad, B. Krishnan, A. Seema, K.R. Dayas, J. Mater. Sci. Mater. Electron. 19 (2008) 1100–1104.
[13] R.E. Mistler, Am. Ceram. Soc. Bull. 69 (1990) 1022–1026.
[14] R. Moreno, Am. Ceram. Soc. Bull. 71 (1992) 1647–1657.
[15] T. Chartier, E. Jorge, P. Boch, J. Eur. Ceram. Soc. 11 (1993) 387–393.
[16] I.R. Oliveria, P. Sepulveda, V.C. Pandolfelli, Am. Ceram. Soc. Bull. 80 (2001) 47–53.
[17] J.J. Guo, J.A. Lewis, J. Am. Ceram. Soc. 83 (2000) 266–272.
[18] K.G. Vasanthakumari, R. Natarajan, Adv. Appl. Ceram. 104 (2005) 73–78.
[19] P. Boch, T. Chartier, Ceram. Int. 4 (1989) 55–67.
[20] S. Bhaskar Reddy, P. Paramanano Singh, N. Raghu, V. Kumar, J. Mater. Sci. 37 (2002) 929–934.
[21] L.C.K. Liau, B. Peters, D.S. Krueger, A. Gordon, D.S. Viswanath, S.J. Lombardo, J. Am. Ceram. Soc. 83 (2000) 2645–2653.
[22] M.J. Cima, J.A. Lewis, A.D. Devoe, J. Am. Ceram. Soc. 72 (1989) 1192–1199.
[23] R.V. Shende, S.J. Lombardo, J. Am. Ceram. Soc. 85 (2002) 780–786.
[24] J.-H. Jean, H.-R. Wang, J. Am. Ceram. Soc. 84 (2001) 267–272.
[25] B. Wong, J.A. Pask, J. Am. Ceram. Soc. 62 (1979) 138–141.
[26] T. Cheng, R. Raj, J. Am. Ceram.Soc. 71 (1988) 276–280.
[27] M.V. Justin, A. Seema, K.R. Dayas, J. Electroceram. 22 (2008) 436–441.
[28] K. Park, I.H. Han, Mater. Sci. Eng. B 119 (2005) 55–60.
[29] K. Park, D.Y. Bang, J. Mater. Sci. Mater. Electron. 14 (2003) 81–87.
[30] K.S. Park, D.Y. Bang, J.G. Kim, J.Y. Kim, C.H. Lee, B.H. Choi, J. Korean Phys. Soc. 41 (2002) 251–256.
[31] K. Park, J. Am. Ceram. Soc. 88 (2005) 862–866.
[32] K. Park, I.H. Han, J. Electroceram. 17 (2006) 1069–1073.
[33] R.S. Roth, Phase Equlibria Diagrams–Phase Diagrams for Ceramists, vol. XI, The American Ceramic Society, Ohio, 1995, p. 10.
[34] G.D.C. Cste de Gyorgyfalva, I.M. Reaney, J. Mater. Res. 18 (2003) 1301–1308.
[35] G.D.C. Cste de Gyorgyfalva, I.M. Reaney, J. Eur. Ceram. Soc. 21 (2001) 2145–2148.
[36] J.A. Kulkarny, V.S. Darshane, Thermochim. Acta 93 (1985) 473–476.
[37] T. Battault, R. Legros, A. Rousset, J. Eur. Ceram. Soc. 15 (1995) 1141–1147.
[38] S.A. Kanade, V. Puri, Mater. Lett. 60 (2006) 1428–1431.
[39] K.H. Zuo, D.L. Jiang, J.-X. Zhang, Q.L. Lin, Ceram. Int. 33 (2007) 477–481.
[40] E.D. Macklen, J. Phys. Chem. Solids 47 (1986) 1073–1079.
[41] O. Bodak, L. Akselrud, P. Demchenmko, B. Kotur, O. Mrooz, I. Hadzaman, O. Shpotyuk, F. Aldinger, H. Seifert, S. Volkov, V. Pekhnyo, J. Alloys Compd. 347 (2002) 14–23.
[42] W.D. Kingery, H.K. Bowen, D.R. Uhlmann, Introduction to Ceramics, second ed., John Wiley & Sons, Singapore, 2004.
[43] W.A. Groen, C. Metzmacher, P. Huppertz, S. Schuurman, J. Electroceram. 7 (2001) 77–87.